DSCC2018-9196

ROBUST FILTERED BASIS FUNCTIONS APPROACH FOR FEEDFORWARD TRACKING CONTROL

Keval S. Ramani

Department of Mechanical Engineering University of Michigan, Ann Arbor, MI, USA ksramani@umich.edu

Chinedum E. Okwudire

Department of Mechanical Engineering University of Michigan, Ann Arbor, MI, USA okwudire@umich.edu

ABSTRACT

This paper proposes a robust filtered basis functions approach for feedforward tracking of linear time invariant systems with dynamic uncertainties. Identical to the standard filtered basis functions (FBF) approach, the robust FBF approach expresses the control trajectory as a linear combination of user-defined basis functions with unknown coefficients. The basis functions are forward filtered using a model of the plant and their coefficients are selected to minimize tracking errors. The standard FBF and robust FBF approaches differ in the filtering process. The robust FBF approach uses an optimal robust filter which is based on minimization of a frequency domain based error cost function over the dynamic uncertainty, whereas, the standard FBF approach uses the nominal model. Simulation examples and experiments on a desktop 3D printer are used to demonstrate significantly more accurate tracking of uncertain plants using robust FBF compared with the standard FBF.

1. INTRODUCTION

Tracking control is a fundamental problem encountered in guiding the motion of systems involved in manufacturing, robotics, aeronautics, and many other industries. The goal of tracking control is to force the output trajectory to follow the desired trajectory as closely as possible. The focus of this paper is feedforward tracking control of linear time invariant (LTI) systems with dynamic uncertainties.

Perfect tracking control (PTC) can be achieved, in theory, by model inversion (i.e., pole-zero cancellation) [1]. PTC results in zero phase and gain errors between the desired and output trajectories, if the plant model is accurate and has a stable inverse. However, when applied to plants with nonminimum phase (NMP) zeros, PTC gives rise to highly oscillatory or unstable control trajectories which are unacceptable. NMP zero are prevalent in practice. For example, they occur in plants with fast sampling rates [2], as well as in plants with noncollocated placement of sensors and actuators [3]. Hence, a lot of research has been done on developing

methods for feedforward tracking control of plants with NMP zeros [4–9].

Recent work by the authors and others [8,10,11] have focused on the filtered basis functions (FBF) approach for feedforward tracking control of NMP systems. The FBF approach can be traced back to work done by Frueh and Phan on plant model inversion in the context of iterative learning control [12]. It assumes that the entire desired trajectory is known a priori and the control input is a linear combination of user-defined basis functions with unknown coefficients. The basis functions are forward filtered through a nominal model of the plant dynamics and the coefficients are selected such that the tracking error is minimized. Unlike many other methods in the literature, the FBF method is also applicable to nonhyperbolic plants (e.g., plants with zero(s) on the unit circle in the z-plane). The tracking performance of the FBF approach does not change significantly with the location of the NMP zero in the z-plane [13], which does not hold for most other tracking controllers. The assumption related to knowledge of the entire desired trajectory was also relaxed using limited preview filtered B-splines (LPFBS) approach [14]. However, since the standard FBF approach relies on a model of the plant, in the presence of uncertainties its accuracy might deteriorate severely.

In their prior work [15], the authors proposed the regularized filtered basis functions approach to improve the accuracy of FBF in the presence of bounded random uncertainties. The regularized FBF approach formulated the coefficient selection problem as a constrained game-type problem where the control objective is to minimize the tracking error in the presence of uncertainties. The solution to the regularized FBF approach is obtained by solving a set of nonlinear coupled equations which is cumbersome as compared to the elegant least squares solution of the FBF approach. For example, the regularized FBF approach is not amenable to the LPFBS algorithm, which is a computationally efficient implementation of the FBF method [14]. An approach that improves robustness of FBF and retains the elegance associated with least squares solution of FBF is therefore desirable. This is

achieved in this paper by replacing the nominal plant model used in standard FBF with a filter which is designed to minimize the effects of dynamic uncertainties on the tracking performance of the FBF approach.

Optimal robust feedforward controllers have been studied in the literature [16,17]. For example, Wu & Zou [16] proposed a gain modulated inversion based controller to minimize the worst-case tracking error in the presence of dynamic uncertainty, which imposes bounds on both magnitude and phase of the uncertainty. Lunenburg [17] discussed an optimal feedforward controller that minimized (in an average sense) the tracking error in frequency domain using a conventional multiplicative uncertainty framework which bounds only the magnitude of the uncertainty. The above mentioned methods [16,17] realized their controllers using a direct inversion method [18]. However, the method [18] is not applicable to nonhyperbolic plants, whereas the FBF approach is.

Therefore, this paper makes the following contributions to the literature:

- 1. The conventional multiplicative uncertainty framework [17], which considers bound on only magnitude, is conservative and hence, this paper considers an alternate dynamic uncertainty framework, which factors in bounds on both magnitude and phase. An optimal feedforward controller that minimizes the tracking error in frequency domain, in the presence of dynamic uncertainties, is designed.
- The inverse of the optimal feedforward controller is used to filter the basis functions and to obtain the filtered basis functions. The coefficients are selected such that the tracking error is minimized in a least squares sense. The resultant method is a more robust version of the standard FBF approach and is denoted as the robust FBF approach.

The effectiveness of the robust FBF approach as compared to the standard FBF approach is demonstrated using simulations and experiments on a desktop 3D printer. This paper is organized as follows. Section 2 gives an overview of the standard FBF approach. Section 3 then introduces the robust FBF approach. Section 4 compares the standard FBF and robust FBF approaches using simulation examples and experiments, followed by conclusions and future work in Sec.

2. OVERVIEW OF THE STANDARD FILTERED BASIS **FUNCTIONS APPROACH**

Consider the discrete-time linear time invariant (LTI) single input single output (SISO) plant G(z) shown in Fig. 1, augmented with a tracking controller, C(z), with overall dynamics L(z) = C(z)G(z) and error dynamics $E_{ff}(z) = 1$ C(z)G(z). The plant G(z) could represent the transfer function of a plant or a closed-loop controlled system [19]. Given a desired trajectory, $y_d(k)$, where $0 \le k \le M$, $k \in \mathbb{Z}$ and M+1 is the number of discrete points in the trajectory, the objective of the tracking controller C(z) is to produce a signal u(k), which after passing

through G(z), results in an output trajectory y(k) that follows the desired trajectory $y_d(k)$ as closely as possible.

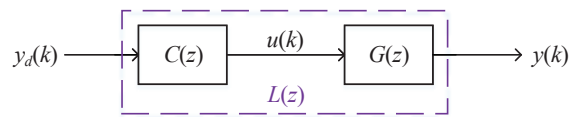


Figure 1: Block diagram for tracking control

The FBF approach assumes that:

- the desired trajectory $y_d(k)$ is known a priori, which is often the case in manufacturing, robotics and aeronautics applications [20]
- b) the control signal u(k) is expressed as a linear combination of basis functions, as follows

$$u(k) = \sum_{i=0}^{n} \gamma_i \varphi_i(k) \tag{1}$$

where $\varphi_i(k)$ and γ_i are the user-defined basis functions and their coefficients, respectively. The control input vector $\mathbf{u} = [u(0)]$ $u(1) \dots u(M)]^{T}$ can be expressed as

$$\mathbf{u} = \mathbf{\Phi} \mathbf{\gamma} \tag{2}$$

where

$$\mathbf{\Phi} = \begin{bmatrix} \mathbf{\phi}_0 & \mathbf{\phi}_1 & \dots & \mathbf{\phi}_n \end{bmatrix}$$

$$\mathbf{\phi}_i = \begin{bmatrix} \varphi_i(0) & \varphi_i(1) & \dots & \varphi_i(M) \end{bmatrix}^{\mathrm{T}}$$
(3)

The resulting output trajectory $\mathbf{y} = [y(0) \ y(1) \ \dots \ y(M)]^T$ can be expressed as a linear combination of filtered basis functions

$$\mathbf{y} = \tilde{\mathbf{\Phi}} \mathbf{\gamma} \tag{4}$$

where $\tilde{\Phi}$ is a $(M+1)\times(n+1)$ matrix whose columns $\tilde{\phi}_i$ are obtained by filtering φ_i using a nominal model, G_{nom} , of the plant G, as shown in Fig. 2. The implication is that the tracking error vector, e, can be expressed as

$$\mathbf{e} = \mathbf{y}_{d} - \tilde{\mathbf{\Phi}} \mathbf{\gamma} \tag{5}$$

where $\mathbf{y}_d = [y_d(0) \ y_d(1) \ \dots \ y_d(M)]^T$. The coefficients γ are selected such that an objective function J, representing the 2norm of the tracking error, is minimized; i.e.

$$\min_{\gamma} \left[J = \|\mathbf{e}\|_{2} = \|\tilde{\mathbf{\Phi}}\gamma - \mathbf{y}_{d}\|_{2} \right]$$
 the result is an optimal coefficient vector, γ , given by

$$\gamma = \left(\tilde{\mathbf{\Phi}}^{\mathsf{T}}\tilde{\mathbf{\Phi}}\right)^{-1}\tilde{\mathbf{\Phi}}^{\mathsf{T}}\mathbf{y}_{d} \tag{7}$$

Remark 1: The standard FBF approach assumes that $G_{nom} = G$, i.e., the nominal model matches the plant perfectly. Hence, E_{ff} = $1 - CG_{nom}$ and minimal E_{ff} can be realized using optimal controller $C_{opt} = G_{nom}^{-1}$. To approximate G_{nom}^{-1} , the standard FBF approach uses G_{nom} to filter the basis functions.

3. ROBUST FILTERED BASIS FUNCTIONS APPROACH FOR TRACKING CONTROL

The previous section assumes that the nominal model, G_{nom} , is a perfect representation of the actual plant, G. However, in practice, $G_{nom} \neq G$, due to uncertainties. In the

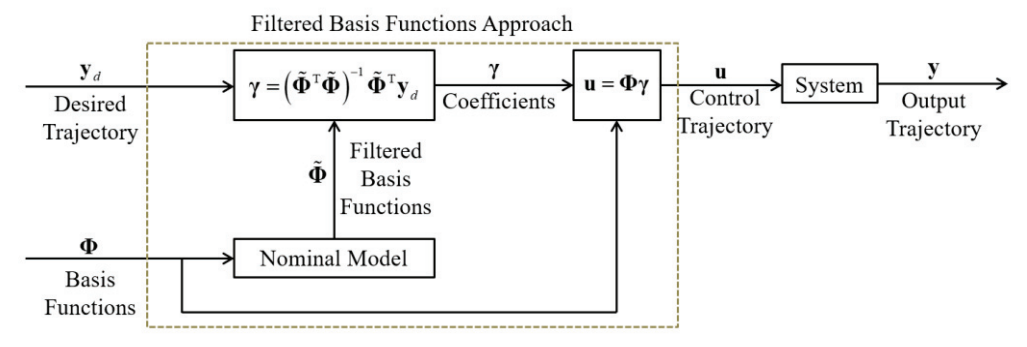


Figure 2: Flowchart for the standard FBF approach

presence of dynamic uncertainties, the actual plant can be expressed as

$$G(e^{j\omega T_s}) = \Delta(e^{j\omega T_s})G_{nom}(e^{j\omega T_s})$$
(8)

based on the substitution $z = e^{j\omega T_s}$, where j is the unit imaginary number, ω is frequency in rad/s and T_s is the sampling time in seconds. The other variables appearing in Eq. (8) are given by

$$\Delta(e^{j\omega T_s}) = r(e^{j\omega T_s})e^{j\theta(e^{j\omega T_s})}$$

$$r_{min}(e^{j\omega T_s}) \le r(e^{j\omega T_s}) \le r_{max}(e^{j\omega T_s})$$

$$\theta_{min}(e^{j\omega T_s}) \le \theta(e^{j\omega T_s}) \le \theta_{max}(e^{j\omega T_s})$$

$$1 < r_{max}(e^{j\omega T_s}) < \infty, \quad 0 \le r_{min}(e^{j\omega T_s}) \le 1$$

$$\theta_{max}(e^{j\omega T_s}) > 0, \quad \theta_{min}(e^{j\omega T_s}) \le 0$$
(9)

 Δ denotes the uncertainty and r and θ are the magnitude and phase of the uncertainty, respectively.

As described in remark 1, in the absence of uncertainties, the standard FBF approach uses inverse of the optimal controller, i.e., G_{nom} , to filter the basis functions. In the presence of dynamic uncertainties (given by Eq. (9)), the optimal controller is the one that minimizes the following cost function (at each frequency ω)

$$J_{r} = \int_{\theta_{min}}^{\theta_{max}} \int_{min}^{r_{max}} f(r, \theta) E_{ff} E_{ff}^{*} r dr d\theta$$
 (10)

where

$$E_{ff} = 1 - C\Delta G_{nom} \tag{11}$$

and $f(r,\theta)$ is the distribution of the dynamic uncertainty w.r.t. to magnitude r and phase θ of the uncertainty, at each frequency ω . Note that, for simplicity, the dependence of $f(r,\theta)$, E_{ff} , r, θ , r_{max} , r_{min} , θ_{max} and θ_{min} on $e^{j\omega T_s}$ is not explicitly shown in Eqs. (10) and (11), and the following equations. The superscript * denotes complex conjugate. The optimal controller can be obtained by differentiating J_r w.r.t. C^* and is given by

$$C_{opt} = G_{nom}^{-1} \int_{\theta_{min}}^{\theta_{max}} \int_{r_{min}}^{r_{max}} f(r,\theta) \Delta^* r dr d\theta$$

$$\int_{\theta_{min}}^{\theta_{max}} \int_{r_{min}}^{r_{max}} f(r,\theta) \Delta \Delta^* r dr d\theta$$
(12)

and hence, the filter for robust FBF is given by

$$G_{r} \doteq C_{opt}^{-1} = G_{nom} \int_{\theta_{min}}^{\theta_{max}} \int_{r_{min}}^{r_{max}} f(r,\theta) \Delta \Delta^{*} r dr d\theta$$

$$\int_{\theta_{min}}^{\pi_{min}} \int_{r_{min}}^{r_{max}} f(r,\theta) \Delta^{*} r dr d\theta$$
(13)

If data about the distribution of uncertainty at each frequency is available, then $f(r,\theta)$ can be used to improve the performance of the optimal controller. Without loss of generality, in the rest of this paper it is assumed that $f(r,\theta) = 1$, i.e., the uncertainty is uniformly distributed. Substituting $f(r,\theta) = 1$ in Eq. (13) gives

$$G_{r} = G_{nom} \frac{3}{4} \frac{r_{max}^{4} - r_{min}^{4}}{r_{max}^{3} - r_{min}^{3}} \frac{\theta_{max} - \theta_{min}}{j(e^{-j\theta_{max}} - e^{-j\theta_{min}})}$$
(14)

The robust filtered basis functions approach filters the user-defined basis functions φ_i using G_r (instead of G_{nom} used by the standard FBF approach), to obtain the filtered basis functions $\tilde{\varphi}_i$. The coefficients are then obtained using the least squares solution given by Eq. (7).

Remark 2: The optimization approach presented above has been used by Lunenburg [17] to find an optimal controller for conventional multiplicative uncertainties, which consider bounds on only the magnitude of the uncertainty. The analysis in this section extends the approach to an alternate dynamic uncertainties framework given by Eq. (9). Wu & Zou [16] designed an optimal controller in the presence of dynamic uncertainties (given by Eq. (9)) using worst case optimization but assumed a gain modulated inversion structure for the controller. Eq. (14) shows that the optimal controller results in both gain and phase modulations of the inverse of the nominal plant.

Typically, during system identification, frequency response functions (FRFs) are generated for different operating conditions. There are various methods to select the nominal model based on the FRFs, for example, selecting any one of the FRFs as the nominal model [14] or using the average of the FRFs as the nominal model [16]. For a given dynamic uncertainty and its distribution, the robust filter (used by robust FBF) is independent of the choice of the nominal model. This is because the robust filter is a result of optimization over the entire uncertainty and invariance of the uncertainty ensures invariance of the robust filter. To prove this, consider two

different nominal models, A and B. The resulting robust filters, based on Eq. (14), are given by

$$G_{r,A} = \underbrace{r_{nom,A}}_{G_{nom,A}} \frac{3}{4} \frac{r_{max,A}^4 - r_{min,A}^4}{r_{max,A}^3 - r_{min,A}^3} \frac{\theta_{max,A} - \theta_{min,A}}{j \left(e^{-j\theta_{max,A}} - e^{-j\theta_{min,A}}\right)}$$

$$G_{r,B} = \underbrace{r_{nom,B}}_{G_{nom,B}} \frac{3}{4} \frac{r_{max,B}^4 - r_{min,B}^4}{r_{max,B}^3 - r_{min,B}^3} \frac{\theta_{max,B} - \theta_{min,B}}{j \left(e^{-j\theta_{max,B}} - e^{-j\theta_{min,B}}\right)}$$
(15)

where

$$r_{nom,A}r_{max,A} = r_{nom,B}r_{max,B}$$

$$r_{nom,A}r_{min,A} = r_{nom,B}r_{min,B}$$

$$\theta_{nom,A} + \theta_{max,A} = \theta_{nom,B} + \theta_{max,B}$$

$$\theta_{nom,A} + \theta_{min,A} = \theta_{nom,B} + \theta_{min,B}$$
(16)

Based on Eqs. (8) and (9), the conditions given by Eq. (16) ensure that the uncertainty region does not change with choice of nominal model. Consider the robust filter for nominal model A

$$G_{r,A} = \frac{3}{4} r_{nom,A} \frac{r_{max,A}^4 - r_{min,A}^4}{r_{max,A}^3 - r_{min,A}^3} \frac{\theta_{max,A} - \theta_{min,A}}{j \begin{pmatrix} e^{-j(\theta_{mix,A} + \theta_{nom,A})} \\ -e^{-j(\theta_{min,A} + \theta_{nom,A})} \end{pmatrix}$$
(17)

Based on Eq. (16),

$$e^{-j(\theta_{\max,A} + \theta_{nom,A})} - e^{-j(\theta_{\min,A} + \theta_{nom,A})}$$

$$= e^{-j(\theta_{\max,B} + \theta_{nom,B})} - e^{-j(\theta_{\min,B} + \theta_{nom,B})}$$
(18)

Also based on Eq. (16),

$$\theta_{max,A} - \theta_{min,A} = (\theta_{max,A} + \theta_{nom,A}) - (\theta_{nom,A} + \theta_{min,A})$$

$$= (\theta_{max,B} + \theta_{nom,B}) - (\theta_{nom,B} + \theta_{min,B})$$

$$= \theta_{max,B} - \theta_{min,B}$$
(19)

Hence,

$$G_{r,A} = \frac{3}{4} r_{nom,A} \frac{r_{max,A}^4 - r_{min,A}^4}{r_{max,A}^3 - r_{min,A}^3} \frac{\theta_{max,B} - \theta_{min,B}}{j(e^{-j\theta_{max,B}} - e^{-j\theta_{min,B}})} e^{j\theta_{nom,B}}$$
(20)

Consider

$$r_{nom,A} \frac{r_{max,A}^{4} - r_{min,A}^{4}}{r_{max,A}^{3} - r_{min,A}^{3}}$$

$$= r_{nom,A} \frac{\left(r_{max,A} - r_{min,A}\right)\left(r_{max,A} + r_{min,A}\right)\left(r_{max,A}^{2} + r_{min,A}^{2}\right)}{\left(r_{max,A} - r_{min,A}\right)\left(r_{max,A}^{2} + r_{max,A}r_{min,A} + r_{min,A}^{2}\right)}$$

$$= \frac{\left(r_{nom,A}r_{max,A} + r_{nom,A}r_{min,A}\right)\left(r_{max,A}^{2} + r_{min,A}^{2}\right)}{\left(r_{max,A}^{2} + r_{max,A}r_{min,A} + r_{min,A}^{2}\right)}$$

$$= \frac{\left(r_{nom,A}r_{max,A} + r_{nom,A}r_{min,A}\right)\left(\left(\frac{r_{max,A}}{r_{min,A}}\right)^{2} + 1\right)}{\left(\left(\frac{r_{max,A}}{r_{min,A}}\right)^{2} + \left(\frac{r_{max,A}}{r_{min,A}}\right) + 1\right)}$$
(21)

Based on Eq. (16),

$$\frac{r_{\max,A}}{r_{\min,A}} = \frac{r_{\max,B}}{r_{\min,B}} \tag{22}$$

hence,

$$\frac{\left(r_{nom,A}r_{max,A} + r_{nom,A}r_{min,A}\right)\left(\left(\frac{r_{max,A}}{r_{min,A}}\right)^{2} + 1\right)}{\left(\left(\frac{r_{max,A}}{r_{min,A}}\right)^{2} + \left(\frac{r_{max,A}}{r_{min,A}}\right) + 1\right)}$$

$$= \frac{\left(r_{nom,B}r_{max,B} + r_{nom,B}r_{min,B}\right)\left(\left(\frac{r_{max,B}}{r_{min,B}}\right)^{2} + 1\right)}{\left(\left(\frac{r_{max,B}}{r_{min,B}}\right)^{2} + \left(\frac{r_{max,B}}{r_{min,B}}\right) + 1\right)}$$

$$= r_{nom,B} \frac{r_{max,B}^{4} - r_{min,B}^{4}}{r_{mon,B}^{3} - r_{min,B}^{3}}$$

$$= r_{nom,B} \frac{r_{max,B}^{4} - r_{min,B}^{4}}{r_{mon,B}^{3} - r_{min,B}^{3}}$$

Substituting Eq. (23) in Eq. (20) gives

$$G_{r,A} = \frac{3}{4} r_{nom,B} \frac{r_{max,B}^{4} - r_{min,B}^{4}}{r_{max,B}^{3} - r_{min,B}^{3}} \frac{\theta_{max,B} - \theta_{min,B}}{j\left(e^{-j\theta_{max,B}} - e^{-j\theta_{min,B}}\right)} e^{j\theta_{nom,B}}$$

$$= \frac{3}{4} r_{nom,B} e^{j\theta_{nom,B}} \frac{r_{max,B}^{4} - r_{min,B}^{4}}{r_{max,B}^{3} - r_{min,B}^{3}} \frac{\theta_{max,B} - \theta_{min,B}}{j\left(e^{-j\theta_{max,B}} - e^{-j\theta_{min,B}}\right)}$$

$$= G_{r,B}$$
(24)

Hence, for a given uncertainty, the robust filter is independent of the choice of the nominal model. Therefore, selection of the nominal model will only affect the performance of the standard FBF and not the robust FBF. The proposed robust FBF approach provides a more methodical approach to the filtering process, in the presence of uncertainties, as compared to the arbitrary selection of nominal model by the standard FBF.

4. EXAMPLES

This section compares robust FBF with the standard FBF approach using simulations and experiments on a HICTOP Prusa i3 desktop 3D printer, shown in Fig. 3. Figure 4 shows the four measured FRFs for the y-axis of the 3D printer. The FRFs are obtained by applying swept sine acceleration signals (with amplitudes ranging from 2 m/s² to 5 m/s²) to the printer's stepper motors (each having 12.5 µm stepping resolution) and measuring the relative acceleration of the build platform and print head using accelerometers (PCB Piezotronics 393B05 and Y356A63). The maximum, minimum and nominal FRFs (shown in Fig. 5) are the maximum, minimum and average of the four FRFs at each frequency, respectively. The FRF for the robust filter is obtained using Eq. (14). To avoid errors associated with fitting a transfer function [14], a frequency domain approach is used to filter the basis functions through the nominal and robust FRFs. The frequency domain approach

uses fft and ifft commands in MATLAB® to filter the basis functions through the dynamics.

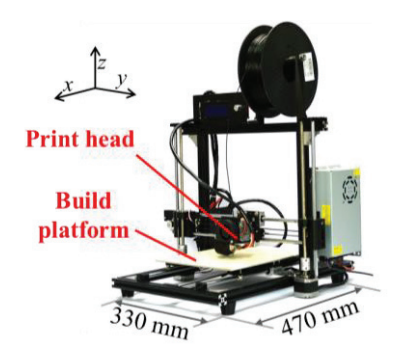


Figure 3: Commercial desktop 3D printer (HICTOP Prusa i3)

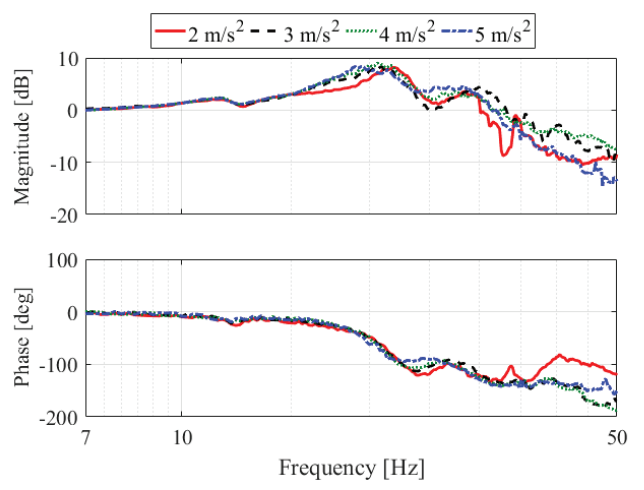


Figure 4: Frequency response functions of y-axis of the 3D printer for various magnitudes of excitation input (acceleration)

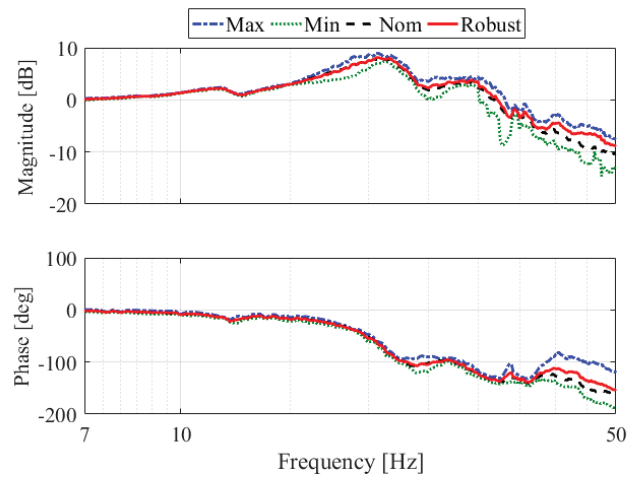


Figure 5: Nominal model (Nom) used for standard FBF with maximum (Max) and minimum (Min) bounds of uncertainty region, the robust filter (Robust) for robust FBF

4.1. SIMULATIONS

As discussed in Secs. 2 and 3, the basis functions are user-defined and there is a wide range of basis functions available for uses with the standard FBF and robust FBF methods; e.g., Laguerre functions [21], wavelets [22], B-splines [10], etc. This paper, uses two rudimentary basis functions: (i) discrete cosine transform (DCT) [23] and (ii) block pulse functions (BPF) [24]. The DCT is a frequency-based transform that is widely used in signal processing; its basis functions are real-valued cosines defined as [23]

$$\varphi_{i}(k) = \beta_{i} \cos\left(\frac{\pi(2k+1)i}{2(M+1)}\right)$$

$$\beta_{i} = \begin{cases} \frac{1}{\sqrt{M+1}} & i = 0\\ \sqrt{\frac{2}{M+1}} & i > 0 \end{cases}$$
(25)

The BPF basis functions are given by

$$\varphi_{i}(k) = \begin{cases}
k \in \left[i\frac{M}{n+1}, (i+1)\frac{M}{n+1}\right], 0 \le i < n \\
k \in \left[i\frac{M}{n+1}, (i+1)\frac{M}{n+1}\right], i = n \\
0 & \text{otherwise}
\end{cases} (26)$$

The BPF expressed in Eq. (26) seeks to divide the time interval from 0 to M among n+1 basis functions in a quasi-uniform manner.

For comparison of robust FBF with standard FBF, four sinusoids with frequencies 30 Hz, 35 Hz, 40 Hz and 45 Hz are used as desired trajectories. The length of each desired trajectory is 5 seconds, resulting in 5001 discrete points (i.e., M = 5000) based on T_s = 1 millisecond. Figure 6 compares the normalized RMS tracking error $(e_{RMS}/y_{d,RMS})$ for the standard FBF and robust FBF approaches, each for 1000 cases (randomly generated with uniform distribution to span the uncertainty region described in Fig. 5); the desired trajectory is a 45 Hz sinusoid and n = 1000 for both DCT and BPF. For both DCT and BPF, it is seen that robust FBF performs better than standard FBF. Table 1 shows the mean normalized RMS tracking errors of the standard and robust FBF (using DCT and BPF, n = 1000) for all the four desired trajectories. For all cases, robust FBF performs better than standard FBF and the percentage improvement in $mean(e_{RMS}/y_{d,RMS})$ varies from 8.46% to 30.38%. Also shown in Tab. 1 is the success rate of robust FBF as compared to standard FBF. The success rate performs a one-on-one comparison between robust FBF and standard FBF for each of the 1000 cases and denotes the number of times robust FBF performs better than standard FBF in terms of $e_{RMS}/v_{d,RMS}$. For the results shown in Fig. 6, the success rate of RFBF is 69.1% (see Tab. 1), for both BPF and DCT, which implies that for 691 of the 1000 cases, $e_{RMS}/v_{d,RMS}$ for robust FBF is lower than $\mathbf{e}_{RMS}/\mathbf{y}_{d,RMS}$ for standard FBF. A success rate higher than 50% for robust FBF as compared to standard FBF, for all desired trajectories, demonstrates that the robust FBF approach is more effective than standard FBF over

Table 1: Comparison of mean normalized RMS tracking errors of standard FBF and robust FBF for four sinusoidal desired trajectories using 1000 cases with dynamic uncertainties, DCT and BPF basis functions (n = 1000). Also, shown is the success rate of robust FBF as compared to standard FBF

Desired	DCT				BPF			
trajectory	$mean(\mathbf{e}_{RMS}/\mathbf{y}_{d,RMS})$		% Improvement in	% Success	$mean(\mathbf{e}_{RMS}/\mathbf{y}_{d,RMS})$		% Improvement in	% Success
frequency	standard	robust	mean($\mathbf{e}_{RMS}/\mathbf{y}_{d,RMS}$)	rate of	FBF	RFBF	$mean(\mathbf{e}_{RMS}/\mathbf{y}_{d,RMS})$	rate of
[Hz]	FBF	FBF	using robust FBF	robust			using robust FBF	robust
			as compared to	FBF			as compared to	FBF
			standard FBF				standard FBF	
30	0.1077	0.0975	9.49	56.9	0.1077	0.0975	9.49	56.9
35	0.1283	0.1175	8.46	65.1	0.1283	0.1175	8.46	65.1
40	0.3947	0.3073	22.15	62.8	0.3947	0.3073	22.15	62.8
45	0.5365	0.3735	30.38	69.1	0.5365	0.3735	30.38	69.1

a wider region of the dynamic uncertainty. So far, the examples used a constant value of n = 1000. The next case considers the effect of number of basis functions on the performance of robust FBF and standard FBF.

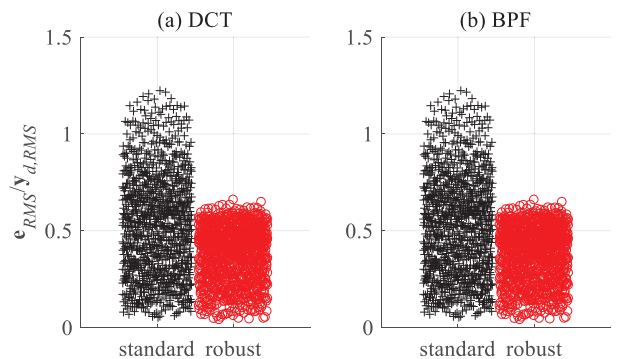


Figure 6: Bee-swarm plots comparing normalized RMS tracking errors of standard FBF and robust FBF for a 45 Hz sinusoidal desired trajectory using 1000 realizations of the actual plant using: (a) DCT and (b) BPF basis functions (both with n = 1000)

In the absence of uncertainty, the performance of standard FBF, in general, improves with increase in number of basis functions and the tracking error converges to 0 as n tends to M. DCT converges monotonically, whereas, BPF does not converge monotonically [8]. Figure 7 shows mean($\mathbf{e}_{RMS}/\mathbf{v}_{d,RMS}$) for robust FBF and standard FBF with DCT and BPF, each for 1000 cases (same as the previous case) as the number of basis functions is varied. The desired trajectory is a 45 Hz sinusoidal signal with M = 5000. As the number of basis functions is increased, mean($e_{RMS}/y_{d,RMS}$) for standard FBF using BPF as well as DCT converges to non-zero values. The difference in converged values for DCT and BPF is negligibly small. A similar behavior is observed for robust FBF and the converged values for robust FBF are lower than the converged values for standard FBF (the values are also shown in Tab. 1). Using DCT, for standard FBF as well as robust FBF, the convergence is monotonic, whereas, for BPF the convergence is not monotonic.

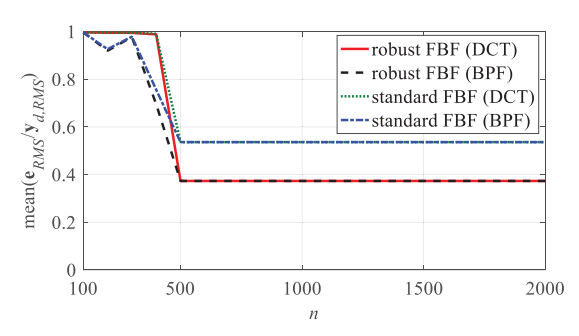


Figure 7: Effect of number of basis functions (DCT and BPF) on mean normalized tracking error performance for standard FBF and robust FBF using 45 Hz sinusoidal desired trajectory and 1000 realizations of the actual plant

4.2. EXPERIMENTS

The standard FBF and robust FBF approaches, with DCT basis functions (n = 1000, M = 5000), are compared using experiments on a HICTOP Prusa i3 desktop 3D printer. Since accelerometers are used as sensors, 45 Hz acceleration signals with varying amplitudes (amplitudes varying from 2 m/s² to 5 m/s² in increments of 0.1 m/s²) are used as desired trajectories for tracking. The variation in amplitude of the desired acceleration signals ensures that a significant portion of the uncertainty (shown in Fig. 5) is spanned. Figure 8 compares the normalized RMS tracking error (e_{RMS}/y_{d,RMS}) for the standard FBF and robust FBF approaches. The mean normalized RMS tracking error mean($\mathbf{e}_{RMS}/\mathbf{y}_{d,RMS}$) for standard FBF and robust FBF are 0.8559 and 0.3604, respectively. The percentage improvement in robust FBF as compared to the standard FBF approach is 57.90% and the success rate is 93.54% (robust FBF performs better than standard FBF in 29 out of 31 cases). The experimental results demonstrate the effectiveness of robust FBF as compared to standard FBF. Note that robust FBF performance as compared to standard FBF is better in experiments then in simulations. This could be attributed to the fact that a large number of uniformly distributed uncertain plant realizations can be generated in simulations, whereas, in experiments the number of realizations of the plant is small and

might not be uniformly distributed. Hence, the difference between simulation and experimental results.

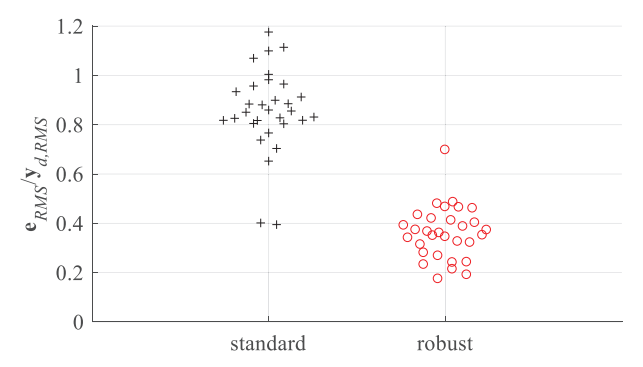


Figure 8: Bee-swarm plots comparing normalized RMS tracking errors of standard FBF and robust FBF in experiments; the desired trajectory is a 45 Hz sinusoid generated using 31 realizations of the dynamics of the 3D printer (obtained by varying the acceleration levels); DCT basis functions (with n = 1000) are used.

5. CONCLUSIONS AND FUTURE WORK

This paper has proposed a robust filtered basis functions approach for tracking control of systems with dynamic uncertainty. The standard filtered basis functions approach uses the nominal model of the plant for filtering. Conversely, the proposed robust FBF approach designs a robust filter for a given uncertainty and its distribution. It is shown analytically that the robust filter does not depend on the choice of the nominal model.

Although the user is free to select any suitable set of basis functions for use with robust FBF, this paper uses the discrete cosine transform (DCT) and block pulse functions (BPF) to compare the standard FBF and robust FBF approaches, using four different sinusoidal desired trajectories. The robust FBF approach is shown to be much more effective than the FBF approach for tracking the uncertain plant. The effect of the number of basis functions on tracking accuracy is also explored and it is observed that robust FBF performs better than FBF for varying number of basis functions. The standard and robust FBF approaches are also compared using experiments on a desktop 3D printer. The experiments also demonstrate the effectiveness of robust FBF as compared to standard FBF. Future work will focus on finding an optimal set of basis functions for tracking systems with dynamic uncertainty.

REFERENCES

- [1] Tomizuka, M., 1987, "Zero Phase Error Tracking Algorithm for Digital Control," J. Dyn. Syst. Meas. Control, **109**(1), pp. 65–68.
- [2] Astrom, K., and Wittenmark, B., 1984, Computer Controlled Systems: Theory and Design, Prentice Hall.
- [3] Miu, D. K., 2012, Mechatronics: Electromechanics and Contromechanics, Springer Science & Business Media.

- [4] Butterworth, J. A., Pao, L. Y., and Abramovitch, D. Y., 2012, "Analysis and Comparison of Three Discrete-Time Feedforward Model-Inverse Control Techniques for Nonminimum-Phase Systems," Mechatronics, 22(5), pp. 577–587.
- [5] Rigney, B. P., Pao, L. Y., and Lawrence, D. A., 2009, "Nonminimum Phase Dynamic Inversion for Settle Time Applications," Control Syst. Technol. IEEE Trans., 17(5), pp. 989–1005.
- [6] Clayton, G. M., Tien, S., Leang, K. K., Zou, Q., and Devasia, S., 2009, "A Review of Feedforward Control Approaches in Nanopositioning for High-Speed SPM," J. Dyn. Syst. Meas. Control, **131**(6), p. 61101.
- [7] Lunenburg, J., Bosgra, O., and Oomen, T., 2009, "Inversion-Based Feedforward Design for Beyond Rigid Body Systems: A Literature Survey," DCT Rep. 2009.105, Eindhoven Univ. Technol. Eindhoven, Netherlands.
- [8] Ramani, K. S., Duan, M., Okwudire, C. E., and Ulsoy, A. G., 2017, "Tracking Control of Linear Time-Invariant Nonminimum Phase Systems Using Filtered Basis Functions," J. Dyn. Syst. Meas. Control. Press, 139(1), p. 11001.
- [9] van Zundert, J., and Oomen, T., 2018, "On Inversion-Based Approaches for Feedforward and ILC," Mechatronics, **50**, pp. 282–291.
- [10] Duan, M., Ramani, K. S., and Okwudire, C. E., 2015, "Tracking Control of Non-Minimum Phase Systems Using Filtered Basis Functions: A NURBS-Based Approach," ASME 2015 Dynamic Systems and Control Conference, American Society of Mechanical Engineers, p. V001T03A006--V001T03A006.
- [11] Kasemsinsup, Y., Romagnoli, R., Heertjes, M., Weiland, S., and Butler, H., 2017, "Reference-Tracking Feedforward Control Design for Linear Dynamical Systems through Signal Decomposition," *American Control Conference (ACC)*, 2017, pp. 2387--2392.
- [12] Frueh, J. A., and Phan, M. Q., 2000, "Linear Quadratic Optimal Learning Control (LQL)," Int. J. Control, 73(10), pp. 832–839.
- [13] Ramani, K. S., Duan, M., Okwudire, C. E., and Ulsoy, A. G., 2018, "A Lifted Domain-Based Metric for Performance Evaluation of LTI and LTV Discrete-Time Tracking Controllers," 2018 International Symposium on Flexible Automation.
- [14] Duan, M., Yoon, D., and Okwudire, C. E., 2017, "A Limited-Preview Filtered B-Spline Approach to Tracking Control with Application to Vibration-Induced Error Compensation of a Commercial 3D Printer," Mechatronics.
- [15] Ramani, K. S., and Okwudire, C. E., 2016, "Regularized Filtered Basis Functions Approach for Accurate Tracking of Discrete-Time Linear Time Invariant Systems with Bounded Random Uncertainties," ASME 2016 Dynamic Systems and Control Conference, American Society of Mechanical

- Engineers.
- [16] Wu, Y., and Zou, Q., 2009, "Robust Inversion-Based 2-DOF Control Design for Output Tracking: Piezoelectric-Actuator Example," IEEE Trans. Control Syst. Technol., 17(5), pp. 1069–1082.
- [17] Lunenburg, J. J. M., 2010, "Inversion-Based MIMO Feedforward Design Beyond Rigid Body Systems," Eindhoven Univ. Technol. Tech. Rep.
- [18] Zou, Q., and Devasia, S., 1999, "Preview-Based Stable-Inversion for Output Tracking of Linear Systems," J. Dyn. Syst. Meas. Control, **121**(4), pp. 625–630.
- [19] Butterworth, J. A., Pao, L. Y., and Abramovitch, D. Y., 2008, "The Effect of Nonminimum-Phase Zero Locations on the Performance of Feedforward Model-Inverse Control Techniques in Discrete-Time Systems," *American Control Conference*, 2008, IEEE, pp. 2696–2702.
- [20] Piegl, L., 1991, "On NURBS: A Survey," IEEE Comput. Graph. Appl., 11(1), pp. 55–71.
- [21] Hamamoto, K., and Sugie, T., 2001, "An Iterative Learning Control Algorithm Within Prescribed Input-Output Subspace," Automatica, **37**(11), pp. 1803–1809.
- [22] Gopinath, S., Kar, I., and Bhatt, R., 2009, "Wavelet Series Based Learning Controller Design for Kinematic Path-Tracking Control of Mobile Robot," *Proceedings of the International Conference on Advances in Computing, Communication and Control*, pp. 129--135.
- [23] Ye, Y., and Wang, D., 2005, "DCT Basis Function Learning Control," Mechatronics, IEEE/ASME Trans., 10(4), pp. 449–454.
- [24] Deb, A., Sarkar, G., and Sen, S. K., 1994, "Block Pulse Functions, the Most Fundamental of All Piecewise Constant Basis Functions," Int. J. Syst. Sci., **25**(2), pp. 351–363.